Medical Mycology, 2015, 53, 477–492
doi: 10.1093/mmy/myv011
Advance Access Publication Date: 7 April 2015
Original Article

Original Article

Transcriptional profile of the human pathogenic fungus *Paracoccidioides lutzii* in response to sulfamethoxazole

Patrícia Fernanda Zambuzzi-Carvalho[1,†], Amanda Gregorim Fernandes[1,†], Marize Campos Valadares[2], Patrícia de Mello Tavares[3], Joshua D. Nosanchuk[3], Célia Maria de Almeida Soares[1] and Maristela Pereira[1,*]

[1]Laboratório de Biologia Molecular, Instituto de Ciências Biológicas, Universidade Federal de Goiás, Goiânia, GO, Brazil, [2]Laboratório de Farmacologia e Toxicologia Celular, Faculdade de Farmácia, Universidade Federal de Goiás, Goiânia, GO, Brazil and [3]Departments of Medicine and Microbiology and Immunology, Albert Einstein College of Medicine, New York, NY, USA

*To whom correspondence should be addressed: Maristela Pereira, Laboratório de Biologia Molecular, Departamento de Bioquímica e Biologia Molecular, Instituto de Ciências Biológicas, ICBII, Campus II, Universidade Federal de Goiás, C.P. 131, 74001-970, Goiânia, GO, Brazil. Tel/Fax: +55 62 35211110; E-mail: maristelaufg@gmail.com
†The authors contributed equally to this work.

Received 15 October 2014; Revised 28 December 2014; Accepted 27 January 2015

Abstract

Paracoccidioidomycosis (PCM) is the most prevalent mycosis in Latin America and is caused by a group of fungi within the *Paracoccidioides* genus. The disease may present clinical and pathological manifestations ranging from asymptomatic pneumonia pulmonary lesions, to disseminated forms involving multiple organs. Sulfonamides were the first drugs used to treat PCM and are still used against this fungal infection. Sulfa drugs are competitive antagonists of ρ-aminobenzoic acid (PABA), a reaction catalyzed by dihydropteroate synthase (DHPS). However, the molecular effects of sulfonamides against the *Paracoccidioides* genus are unknown. The aim of this work was to investigate the global mechanism of action of sulfamethoxazole on *Paracoccidioides lutzii*. Yeast cells were grown on minimum medium in the presence or absence of sulfamethoxazole to construct EST libraries. The representational difference analysis (RDA) technique was used to identify up- and down-regulated *P. lutzii* genes after treatment with sulfamethoxazole. Approximately six transcripts related to mitochondrial function were differentially expressed. To confirm the RDA and bioinformatics results, several relevant genes were studied with quantitative real-time polymerase chain reaction (qRT-PCR) to evaluate their levels of expression. To confirm the impact of sulfamethoxazole on mitochondria, we measured the reduction of tetrazolium salt 3-(4,5-dimethylthiazol-2-yl)-2,5-diphenyltetrazolium bromide (MTT) by *P. lutzii* with or without exposure to the drug. MTT assays reveal that sulfamethoxazole produces a marked dose-dependent adverse

effect on *P. lutzii*. The transcriptional activity of selected genes in infected macrophages corroborated our *in vitro* results. The results indicated that sulfamethoxazole acts in *P. lutzii* as a competitor for amino acid, nucleic acids and folate cofactor biosynthesis, disrupting mitochondrial functions.

Key words: *Paracoccidioides lutzii*, sulfamethoxazole, representational difference analysis, transcriptome, antifungal.

Introduction

Paracoccidioidomycosis (PCM), the most prevalent mycosis in Latin America [1], is caused by at least two different species complexes: *Paracoccidioides brasiliensis* (harboring S1, PS2, PS3, and PS4 cryptic species) and *Paracoccidioides lutzii*. *P. lutzii* was recently proposed as a new species within the *Paracoccidioides* genus using molecular and morphological approaches [2,3]. In Brazil, approximately 50% of the deaths caused by systemic mycoses between 1996 and 2006 were due to the *Paracoccidioides* genus [4]. The disease causes a broad spectrum of clinical and pathological manifestations, ranging from asymptomatic pulmonary lesions and mild respiratory infections to life-threatening disease that can involve multiple organs, most often the lungs, oropharyngeal mucosa, skin, lymph nodes, adrenal glands, and the central nervous system [5].

Antifungal chemotherapy is required for PCM, although complete eradication of the fungus may not occur even after long-term therapy. Initial treatment depends on the severity of the disease and varies from 2 to 6 months; therapeutic options include sulfonamides, amphotericin B, and azoles. Extended periods of treatment are often necessary, up to 2 or more years, and relapsing disease frequently occurs [6,7]. In the 1940s, sulfonamides were determined to be the first effective drug for the treatment of PCM [8], and they continue to be used as standard treatment today, including for the severe childhood forms [6,9].

Sulfa drugs are competitive antagonists of ρ-aminobenzoic acid (PABA) [10], which is condensed with 2-amino-4-hydroxy-6-hydroxymethyl-7,8 dihydropteridine pyrophosphate (DHPPP) to form dihydropteroate (DHP), a reaction catalyzed by dihydropteroate synthase (DHPS). DHPS is a key enzyme involved in folate synthesis [11]. Folate cofactors are involved in the biosynthesis of purines and pyrimidines (thymidylate), in the biosynthesis of amino acids such as glycine and methionine, and in the biosynthesis of vitamins such as pantothenic acid [12]. However, the mechanisms of action of sulfonamides on the fungal pathogen *Paracoccidioides lutzii* have not been defined.

Several studies of antifungal agents have identified genes that respond to these compounds [13,14]. We use representational difference analysis (RDA) as optimized by Pastorian et al. [15] to identify genes that are differentially expressed by *P. lutzii* under different growth conditions [16–21]. RDA is a sensitive and powerful tool for the identification of up- and down-regulated genes in two different populations of cDNA [22].

The aim of this study was to assess the global response of *P. lutzii* to the effects of sulfamethoxazole. Using the RDA approach, we identified genes that were differentially expressed in *P. lutzii* in response to exposure to a sub-inhibitory concentration of sulfamethoxazole. The data were confirmed by quantitative real-time polymerase chain reaction (qRT-PCR) and reduction of tetrazolium salt 3-(4,5-dimethylthiazol-2-yl)-2,5-diphenyltetrazolium bromide (MTT). In addition, the transcript levels of selected genes were also measured during *ex vivo* macrophage infection. These changes in the gene expression profile provided insights into the mechanism of action of sulfamethoxazole on *P. lutzii* (formerly *Paracoccidioides brasiliensis*, isolate 01).

Materials and methods

P. lutzii culture and determination of cell viability

*P. lutzii Pb*01 (ATCC MYA-826) has been extensively studied in our laboratory [23–26]. *P. lutzii* yeast cells were sub-cultured every seven days on semi-solid Fava-Netto's medium [1% (w/v) peptone; 0.5% (w/v) yeast extract; 0.3% (w/v) proteose peptone; 0.5% (w/v) beef extract; 0.5% (w/v) NaCl; 4% (w/v) glucose; 1% (w/v) agar, pH 7.2] [27] at 36°C and used throughout this study.

The determination of IC_{50} was performed according to Santo et al. [28]. The experiments were processed in triplicate. For viability experiments, yeast cells were grown in the presence or absence of 0.01 mg/mL (IC_{50}) of sulfamethoxazole, in liquid minimal medium McVeigh Morton (MMcM) [29] at 36°C, and the viability of the cells at different time intervals was determined by the trypan blue method [30]. In brief, cells were incubated with a dye solution (0.1% trypan blue stain) for 5 min at room temperature and viability was assessed by counting viable and dead cells in a Neubauer chamber.

RNA isolation and cDNA synthesis

P. lutzii yeast cells were grown in liquid Fava-Netto's medium for 72 h and then transferred to the liquid MMcM

for 16 h. Then, *P. lutzii* yeast cells were grown in liquid MMcM for 1 h and 2 h in the presence and absence of 0.01 mg/mL sulfamethoxazole, and total RNA was extracted using Trizol (Invitrogen, Carlsbad, CA, USA) according to the manufacturer's instructions. The RNA was treated with RNAse-free DNAse I (Invitrogen) to remove chromosomal DNA. RNA purity was assessed by spectrophotometry using the A_{260nm}/A_{280nm} ratio and the integrity was inspected by 1.5% gel electrophoresis. The RNAs were used to construct subtracted cDNA libraries. The first-strand cDNA was synthesized from 1 μg of DNAse-treated RNAs using reverse transcriptase (RT Superscript III, Invitrogen) and used as a template to synthesize the second-strand using the SMART PCR cDNA synthesis kit (Clontech Laboratories, Palo Alto, CA, USA).

J774 A.1 mouse macrophage cells culture and infection with *P. lutzii*

The J774 A.1 mouse macrophage-likes cells were obtained from the Rio de Janeiro Cell Bank (Rio de Janeiro, Brazil) and maintained an atmosphere of 5% carbon dioxide at 37°C in RPMI 1640 medium supplemented with 10% heat-inactivated fetal bovine serum (Vitrocell/Embriolife, Campinas, SP, Brazil), 10% amino acid solution (Sigma Biochemical, St. Louis, MO, USA) and 0.2% gentamicin solution (Sigma Biochemical).

The macrophages cells were quantified by counting in a Neubauer chamber, plated at 10^6 cells per well on glass coverslips in 24-well culture plates and infected with 2.5×10^6 *P. lutzii* yeast cells, also determined by counting in a Neubauer chamber. The cells were co-cultured for 24 h in the presence of 0.01 mg/ml of sulfamethoxazole at 37°C in 5% CO_2 to allow fungal internalization. The supernatants were removed, and the cell layer was observed using light microscopy, to visualize fungal cells internalized by the macrophage. In addition, the number of viable fungi co-cultivated with the macrophages was determined by quantifying the number of colony-forming units (CFUs). In other wells, the monolayers were gently washed with 1X phosphate-buffered saline (PBS) to remove any nonadherent/internalization yeast cells, and the total RNA was isolated as described above.

RDA methodology

The cDNA libraries were generated using the RDA technique [15] with minor modifications. This subtractive hybridization strategy removes transcripts shared by the driver and tester populations and enriches the tester library for differentially expressed genes. Double-stranded cDNAs (1 μg) were digested with *Sau3*AI restriction enzyme (Amersham Biosciences, Little Chalfont, Uppsala, Sweden). The digestion products were linked to adapter primers and PCR-amplified to generate cDNAs representations for the driver and tester. Two successive rounds of PCR amplifications employing different adapters (J-Bam and N-Bam, Table 2) were performed to enrich the differentially expressed sequences. In the first round, we hybridized the tester/driver at a ratio of 1:10; in the second round the tester/driver ratio was set at a higher stringency of 1:100. Before each round of hybridization, the cDNAs were purified using the GFX PCR purification kit (GE Healthcare UK, Little Chalfont, Buckinghamshire, England). In the RDA method, cDNA from yeast cells cultured in MMcM broth medium with 0.01 mg/ml of sulfamethoxazole for 1 and 2 h served as the tester population. They were hybridized to cDNA from yeast cells cultured in MMcM broth medium only, for 1 and 2 h as driver, and vice versa. This resulted in four differential expression libraries, two for up-regulated transcripts and two for down-regulated transcripts. The adapters used for subtractive hybridizations are listed in Table 2.

The cDNAs from these libraries were cloned into a pGEM-T Easy vector (Promega, Madison, WI, USA) that was used to transform *Escherichia coli* XL1 Blue electro competent cells. The positive colonies were picked and grown in deep-well plates. The plasmid DNA was purified by a miniprep protocol (Qiagen, Venlo, Netherlands, Germany) and was used as the template in the standard fluorescence labeling dye-terminator protocols with a T7 flaking vector primer. The reaction products were loaded onto a MegaBACE 1000 DNA sequencing system (GE Healthcare) for automated sequence analysis.

Bioinformatics analysis

The reading quality of the sequences was checked by the Phred program module [31], and we analyzed the sequences with at least 50 nucleotides and a quality grater or equal to 20. Then, the vector sequences were timed using the Cross-match program [32]. Subsequently, the sequences were assembled using the CAP3 program [33] to obtain the final set of contigs and singlets. All these tools were integrated in a specific pipeline [34]. A search for functional categories was performed using the program Blast2GO [35] that provides a comparison between clusters of sequences obtained from public databases. The BLAST program of the National Center for Biotechnology Information (NCBI) [36] processed with non-redundant sequences (nr) GenBank and the nucleotide database generated from the *P. lutzii* structural genome [37] were used for the annotation of the ESTs. The database sequence matches were considered significant at e-values $\leq 10^{-5}$ with sequence coverage cuts of 39.7%.

The program INTERPROSCAN [38] was used to obtain information about the classification of families. The metabolic pathways were analyzed using maps obtained from the KEGG database (Kyoto Encyclopedia of Genes and Genomes) [39] with annotated EC numbers, and this information was used to help elucidate the function of the ESTs. The Munich Information Center for Protein Sequences (MIPS) [40] was used to designate the functional categories.

Sequence analysis and the annotation pipeline were set up using the Blast2GO program, which joins in one GO application a similarity search with statistical analysis and highlighted visualization on a directed acyclic graph [41]. The Blast2GO annotation algorithm takes multiple parameters into account such as sequence similarity, blast HSP (highest scoring pair) length and *e-values*, the GO hierarchical structure and the GO term evidence codes [41,42].

For GO functions with up- or down-regulated genes, graphs were plotted for the times of exposure to the compound to demonstrate the statistically enriched genes of each functional category (Supplementary Fig. 1). The percentage of the occurrence of each gene in relation to the total number of genes from the libraries was calculated and is shown in Supplementary Table 1.

Quantitative real-time PCR (qRT-PCR)

Total RNAs from *P. lutzii* yeast cells cultured in the presence or absence of sulfamethoxazole were obtained as previously described in independent experiments from those used in the RDA assays. After treatment with DNAse, first strand cDNAs were synthesized from total RNA using Superscript II reverse transcriptase (Invitrogen) and an oligo $(dT)_{15}$ primer according to the supplier's instructions. Gene-specific primers were designed for the gene of interest and for the gene α-tubulin using Primer Express software (Applied Biosystems, Foster City, CA, USA). The qRT-PCRs were performed in triplicate in a StepOnePlus™ real-time PCR system (Applied Biosystems). The PCR thermal cycling program consisted of 40 cycles of 95°C for 15 s and 60°C for 1 min.

The SYBR green PCR master mix (Applied Biosystems) was used for each reactions and was supplemented with 1 ρmol of each gene-specific oligonucleotides and 40 ng of template cDNA in a final volume of 20 µl. A melting curve analysis was performed to confirm the amplification of a single PCR product. The data were normalized to the α-tubulin gene of *P. lutzii*. A nontemplate control was included. A cDNA for a relative standard curve was generated using an aliquot of cDNA from each sample. Relative expression levels of the genes of interest were calculated using the standard curve method for relative quantification [43]. Student's *t*-test was used for statistical comparisons and *P* values $\leq .05$ were considered statistically significant. The specific sense and antisense primers are listed in Table 2.

Assessment of mitochondrial activity of *P. lutzii* by MTT

P. lutzii yeast cells (1×10^6 cells/well) were seeded in a 96-well plate (TPP, Trasadingen, Zürich, Schweiz), and incubated with different concentrations of sulfamethoxazole (1.28, 0.64, 0.32, 0.16, 0.08, 0.04, 0.02, and 0.01 mg/ml) in sextuplicate. After incubation at 36°C for 120 h, in a shaker at 180 rpm, 20 μl of MTT (Sigma-Aldrich) at 5 mg/ml was added to each well, and the plate was incubated for 4 h at 36°C. The plate was then centrifuged at 800 rpm for 10 min, and the supernatant was removed. Next 100 μl of dimethyl sulfoxide (DMSO) (Vetec, Rio de Janeiro, RJ, Brazil) was added to each well for solubilization of formazan crystals; the plate was gently homogenized and the concentration of solubilized formazan was quantified spectrophotometrically using an ELISA reader (Stat Fax 2100, Awareness Technology, Dusseldorf, Germany) at a wavelength of 540 nm. The absorbance of control cells (untreated) was considered 100% cell viability; the white (medium control) contained only DMSO. The cytotoxicity of the compound was calculated as follows:

$$\text{Viability} = \frac{\text{Mean absorbance for each concentration of the extract} - \text{white} \times 100}{\text{Mean absorbance of control} - \text{white}}$$

The MTT test was performed in triplicate, and each concentration of sulfamethoxazole was assessed in sextuplicate. The results of viability were plotted (Graphpad Prism 5.0, Software, San Diego, CA, USA).

Fluorescence microscopy

The fungus was subcultured at 36°C on Sabouraud solid medium for 6 days and transferred to Fava-Netto liquid medium for 72 hours. Thereafter, the fungus was transferred to MMcM for 16 hours. An aliquot of 10^6/ml of *P. lutzii* yeast cells was added to MMcM containing three different concentrations of sulfamethoxazole: 0.64g/ml, 0.08 mg/ml and 0.01 mg/ml (at final volume of 200 µl). After 24 h and 48 h of treatment, the cells were stained

with 10 μM FUN-1 (Life Technologies) and viewed with an Olympus AX70 microscope with a 4′,6-diamidino-2-phenylindole (DAPI) fluorescence filter [44].

Results

Generation of RDA products

cDNA libraries were constructed using 0.01 mg/ml sulfamethoxazole, which corresponds to the IC_{50} for *P. lutzii*, at 1 and 2 h of incubation at 36°C. Cell viability was ∼ 85% (data not shown). The libraries were constructed using the RDA technique as described [15]. Amplification of two rounds of RDA revealed different banding patterns of amplified fragments within each time interval (data not shown). After total RNA extraction and RDA assay, the differential products were isolated and cloned in a pGEM-T Easy vector and sequenced.

Global gene expression profile

A total of 683 ESTs were successfully sequenced and differentially regulated. From these, 77 and 187 up- and down-regulated genes, respectively, were obtained from *P. lutzii* yeast cells after incubation with sulfamethoxazole for 1 h; and 177 and 242 up- and down-regulated genes, respectively, after 2 h of incubation. For the library of up-regulated genes after 1 h of exposure of the fungus to sulfamethoxazole, a total of 16 genes were grouped into 20 clusters with 11 contigs and 9 singlets after pipeline analysis. For the library of up-regulated genes after 2 h, a total of 11 genes were grouped into 25 clusters with 12 contigs and 13 singlets. For the library of down-regulated genes after 1 h of exposure, a total of 34 genes were grouped into 52 clusters with 23 contigs and 29 singlets. For the library of down-regulated genes after 2 h, a total of 11 genes were grouped into 33 clusters with 16 contigs and 17 singlets. The ESTs were submitted to the National Center for Biotechnology Information (NCBI) under the following accession numbers: LIBEST_028467 *Paracoccidioides* sulfamethoxazole 1 h up Library, LIBEST_028466 *Paracoccidioides* sulfamethoxazole 1 h down Library, LIBEST_028469 *Paracoccidioides* sulfamethoxazole 2 h up Library and LIBEST_028468 *Paracoccidioides* sulfamethoxazole 2 h down Library. The RDA data from this study are available on the EST database (dbEST) at = under series.

The differentially expressed genes were compared to *P. lutzii* genes in the Broad Institute database by Blast X. ESTs with an e-value $< 10^{-5}$ were identified. The contigs and singlets were annotated using the Blast2GO program. The classification by functional category and the general distribution of genes among various functional groups was obtained based on this annotation, according to the classification of GO (Table 1).

The GO functions with up- or down-regulated genes after exposure to sulfamethoxazole were plotted in graphs to demonstrate the statistically enriched function (Supplementary Fig. S1). The groups with the highest percentage of up-regulated genes were the cell rescue, defense and virulence (65%), metabolism (20%), cellular transport, transport facilities and transport routes, and unclassified proteins (6%), unclassified proteins (4%), transcription (2%), energy, protein fate and functional unclassified proteins (1%). The highest percentage of down-regulated genes were grouped in the metabolism (44%), transcription (20%), energy (11%), cell rescue, defense and virulence (10%), cell cycle and DNA processing, functional unclassified proteins and unclassified proteins (3%) and cellular transport, transport facilities and transport routes, protein synthesis, and protein fate (2%) groups.

The distribution of differentially expressed genes in biological functional groups was evaluated (Table 1; Fig. 1A and 1B). From this analysis, we observed that most of the genes down-regulated after 1 h of incubation participated in cellular processes related to transcription and cell rescue, defense and virulence. On the other hand, the up-regulated genes primarily functioned in metabolism, cellular transport, transport facilities and transport routes. After 2 h, most of the down-regulated genes were involved in metabolism and the up-regulated genes were related to cell rescue, defense and virulence. The percentage of occurrence of each gene in the libraries is indicated in Supplementary Table S1.

Some genes from the respiratory complex group, such as ATP synthase subunit β (ATP2) and carnitine/acyl carnitine carrier (ACUH), as well as acyl-CoA dehydrogenase (ACAD) from β-oxidation, were down-regulated. Many genes involved in cell rescue, defense and virulence or cellular transport were up-regulated; for example, various heat shock proteins, and the major facilitator superfamily transporter (MFS) and the ABC transporter.

Treatment with sulfamethoxazole resulted in up-and down-regulated genes involved in different biological processes (Table 1; Fig. 2). Among potentially relevant genes and those that had more representation in the number of ESTs in response to sulfamethoxazole after 1 h of treatment that could be cited as up-regulated was cysteine desulfurase (NFS1). The down-regulated genes included C6 transcription factor (CTF1B), betaine aldehyde dehydrogenase (BADH), heat shock protein (HSP30), GATA-type sexual (NSDD), carnitine/acyl carnitine carrier (ACUH) and ribonuclease reductase large subunit (RNR1).

Table 1. Annotated ESTs up- and down-regulated genes of *Paracoccidioides* yeast cells treated with Sulfamethoxazole by 1 and 2 h.

Functional category	Gene product	*Paracoccidioides* acession number[a]	e-value	Number of occurrence 1 h	Number of occurrence 2 h
Metabolism					
Amino acid metabolism	Glutamine synthetase (GLN1)	PAAG_07003.1	0.0		+3
Carbohydrate metabolism	Betaine aldehyde dehydrogenase (BADH)	PAAG_05392.1	0.0	−22	−161
	Cysteine desulfurase (NFS1)	PAAG_05850.1	3e-122	+44	+3
	Dolichyl pyrophosphate Man9GlcNAc2 α-1,3-glucosyltransferase (ALG6)	PAAG_01732.1	3e-86	−1	
	Trehalose phosphatase (TPS1)	PAAG_06703.1	9e-115	+1	
Fatty acid metabolism	NADPH dehydrogenase (OYE)	PAAG_08159.1	0.0	−1	
	Fatty acid elongase (GNS1/SUR4)	PAAG_08553.1	5e-131	+1	−1
	Hemolysin – III (HLY-III)	PAAG_01871.1	0.0	−1	
Ubiquinone metabolism	3-demethylubiquinone-9 3-methyltransferase (COQ3)	PAAG_06595.1	8e-121	−1	
Energy					
Pentose-phosphate pathway	Ribulose-phosphate 3-epimerase (RPE1)	PAAG_01632.1	0.0	+2	
Respiration	Carnitine/acyl carnitine carrier (ACUH)	PAAG_03452.1	9e-138	−15	−29
	ATP synthase subunit β (ATP2)	PAAG_08037.1	0.0	−1	
Fatty acid β-oxidation	Acyl-CoA dehydrogenase (ACAD)	PAAG_01222.1	3e-53	−1	
Transcription	C6 transcription factor (CTF1B)	PAAG_01359.1	0.0	−35	−25
	Pirin (PIR)	PAAG_04726.1	4e-36	−5	
	Cross-pathway control protein A	PAAG_03094.1	6e-140		+1
	tRNA methyltransferase complex (TRM10)	PAAG_04192.1	9e-170	−2	
	GATA-type sexual (NSDD)	PAAG_05818.1	0.0	−16	
	Histone deacetylase (RPD3)	PAAG_06742.1	0.0	−1	+1
	RING finger protein (RNF)	PAAG_06129.1	1e-165	+2	
	Transcription factor (STEA)	PAAG_00406.1	0.0	+1	−2
	Trancription factor C_2H_2 (SEB1)	PAAG_07831.1	0.0	−1	
Protein fate	Ubiquitin thioesterase (OUT1)	PAAG_08841.1	2e-111	+2	
	Ubiquitin (UBI)	PAAG_07080.1	3e-104	−1	
	Ubiquitin interaction motif protein (S5a)	PAAG_04028.1	2e-99	−1	
	Dipeptidase (DPEP)	PAAG_02915.1	5e-178	−1	
	Guanine nucleotide binding protein α-1 subunit (GPA2)	PAAG_04436.1	2e-90	−2	−3
Protein synthesis	ATP-dependent RNA helicase (eIF-4A)	PAAG_00689.1	2e-78	−8	−2
Cellular transport, transport facilities and transport routes	Succinate/fumarate mitochondrial transporter (ACR1)	PAAG_06563.1	1e-150	−2	+2
	ABC transporter	PAAG_04548.1	1e-172	+1	
	ADP/ATP carrier protein (AAC)	PAAG_08620.1	2e-83	+1	
	Dicarboxylic amino acid permease (DIP5)	PAAG_04187.1	5e-95	−4	
	Stomatin family protein	PAAG_06541.1	1e-125	−1	
	Vesicular-fusion protein (SEC17)	PAAG_06233.1	2e-159	−1	
	Major facilitator superfamily transporter (MFS)	PAAG_01353.1	0.0	+9	+1
Cell cycle and DNA processing	Ribonuclease reductase large subunit (RNR1)	PAAG_02210.1	3e-111	−12	
	β-lactamase family protein (PSO2)	PAAG_01244.1	7e-77	−1	

Table 1. *Continued*

Functional category	Gene product	*Paracoccidioides* acession number[a]	e-value	Number of occurrence 1 h	Number of occurrence 2 h
Cell rescue, defense and virulence					
Stress response	Survival factor 1 (SVF1)	PAAG_02425.1	2e-89	−1	
	Heat shock protein (HSP)	PAAG_05679.1	5e-128	−3	
	Heat Shock Protein (HSP60)	PAAG_08059.1	0.0		+59
	Heat shock protein (HSP70)	PAAG_08003.1	0.0	−3	+89
	Heat Shock Protein (HSP88)	PAAG_07750.1	2e-152		+3
	Heat shock protein (HSP30)	PAAG_00871.1	0.0	−30	+14
	Phospholipase D (SPO14)	PAAG_00220.1	8e-76	−2	
Virulence factor	Pathogenesis associated protein (CAP20)	PAAG_06538.1	0.0		−2
	GTP-binding protein (RHO2)	PAAG_01879.1	1e-87	+1	
Biogenesis of cellular components	Transmembrane GTPase (FZO1)	PAAG_02592.1	6e-175	−1	
Cell fate	DHHC zinc finger membrane protein	PAAG_06616.1	5e-150	−2	
Functional unclassified proteins	Pleckstrin Homology domain (PH)	PAAG_03092.1	0.0	+3	−10
	DUF 1688 domain protein	PAAG_04190.1	0.0	−1	−1
Unclassified proteins	Conserved hypothetical protein	PAAG_05467.1	1e-159	−4	
	Conserved hypothetical protein	PAAG_02735.1	8e-127	+2	
	Hypothetical protein	PAAG_03092.1	0.0	−2	
	Hypothetical protein	PAAG_06820.1	0.0	+3	−6
	Hypothetical protein	PAAG_05009.1	4e-151	+3	
	Hypothetical protein	PAAG_01099.1	8e-116	+1	
	Hypothetical protein	PAAG_07684.1	6e-159	−1	
	Hypothetical protein	PAAG_04118.1	4e-64		+1

[a]Accession number at Broad (http://www.broadinstitute.org).

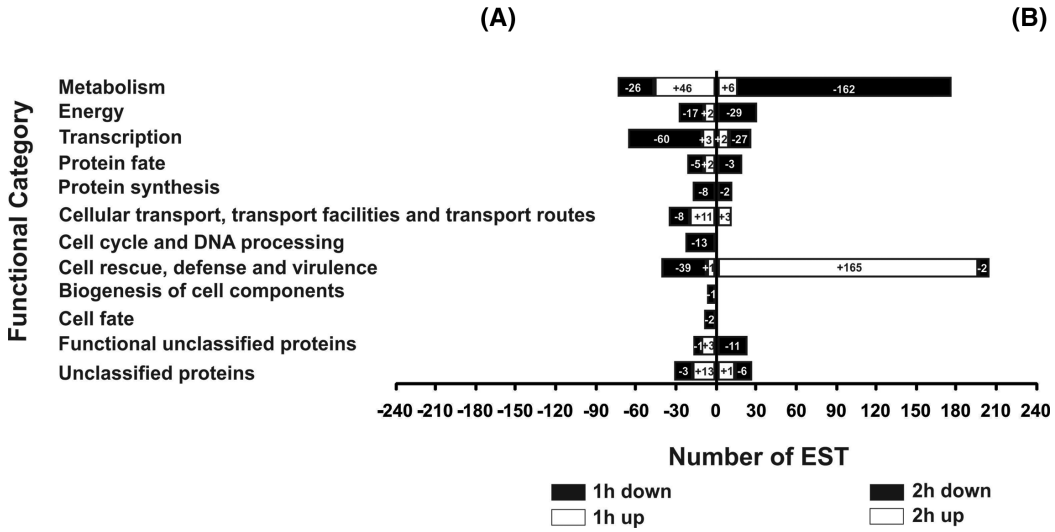

Figure 1. Functional classification of differentially expressed genes in biological functional groups. *P. lutzii* yeast cells were treated with sulfamethoxazole for 1 h (A) or 2 h (B) and gene expression was compared to untreated cells. The numbers of ESTs are indicated with black bar segments for the down-regulated genes and white bar segments for the up-regulated genes. The numbers of ESTs of each category are shown (see Table 1). The functional classification was based on homology of each EST against the GenBank non-redundant database at a significant homology cut-off $\leq 1e^{-05}$ and on the MIPS functional annotation scheme. Each functional class is represented as a segment and is expressed as the number of ESTs in each library.

Table 2. Oligonucleotides primers used in RDA assay and qRT-PCR.

Sequence Name	Foward primer (5′-3′)	Reverse primer (5′-3′)	Reaction
cDNA	AGCAGTGGTATCAACGCAGAGTACGCGGG		Synthesis of the first-strand for RDA
CDS	AAGCAGTGGTATCAACGCAGAGTACT (30) N1N[a]		Synthesis of the first-strand for RDA
PCRII	AAGCAGTGGTATCAACGCAGAGT		Synthesis of the second-strand for RDA
JBam12,24	GATCCGTTCATG	ACCGACGTCGACTATCCATGAACG	Adapter 1 (RDA)
NBam12,24	GATCCTCCCTCG	AGGCAACTGTGCTATCCGAGGGAG	Adapter 2 (RDA)
T7	GTAATACGACTCACTATAGGGC		Sequencing
Oligo (dT)15	AAGCAGTGGTATCAACGCAGAGTACT(30)N1N3′		Synthesis of the first0strand for qRT-PCR
Glutamine Synthetase (GLN1)	CGATCAAAAACAAAGACCCT	GGTCTGGGTACATGGCAAC	qRT-PCR
ATP synthase subunit β(ATP2)	GCTATGGATGGTACCGAGG	TTGATACCAGTAACCAGGAC	qRT-PCR
Succinate/Fumarate mitochondrial transporter (ACR1)	GGGGTAAAACCTCGAGGCTT	AAAGTTGTCCGGTCTCCTTGT	qRT-PCR
Acyl-CoA dehydrogenase (ACAD)	GAGAACGAGACGCCCGAAG	GTTGTAGTAAGGACTCTTGTAG	qRT-PCR
3-demethylubiquinone-9 3-methyltransferase (COQ3)	CCCTCACACAAATCCACATC	TGTCCGTCGATAATGAATGAGA	qRT-PCR
Ubiquitin (UBI)	GGAGGCATGCAGATCTTCGT	ACGACCGTCCTCAAGCTGC	qRT-PCR
Carnitine/Acyl-Carnitine carrier (ACUH)	GAAGGCATTGCCAGGGGT	CATTATGAACGGGGACGGTG	qRT-PCR
NADPH dehydrogenase (OYE)	GGGCTGTCTCCACTATGTCA	CGCTGCTTCCGTCATGATAAA	qRT-PCR
Transmembrane GTPase (FZO1)	CATGTCCATCAATTGTTATACAA	ATCTCACTCCCATCCATCGC	qRT-PCR
Dihydropteroate synthase (DHPS)	TGCGACCGCTTTGCCAACTT	GGGTGAGGCGTGGGAGATG	qRT-PCR
Dihydrofolate reductase (DHFR)	CTTCGACGGGGTAATTGGCT	GCAGTGGTTGTGGTGGTGAT	qRT-PCR

[a](N1 = A, G or C / N = A, C, G or T)

Similarly, treatment with sulfamethoxazole for 2 h also revealed up-and down-regulated genes involved in different biological processes (Table 1; Fig. 2). After 2 h of treatment with sulfamethoxazole, the up-regulated genes included those for heat shock protein (HSP70), heat shock protein (HSP60), and heat shock protein (HSP30). The down-regulated genes included betaine aldehyde dehydrogenase (BADH), carnitine/acyl carnitine carrier (ACUH), guanine nucleotide binding protein α-1 subunit (GPA2), C6 transcription factor (CTF1B) and pleckstrin homology domain (PH) (Table 1; Fig. 2).

Analysis of RNA transcripts by qRT-PCR

To confirm the data from RDA libraries, the transcriptional levels of selected genes related to mitochondrial functions and cellular metabolism, including β-oxidation, that were identified as regulated by RDA analysis were measured by qRT-PCR. Target genes included ATP2, transmembrane GTPase (FZO1), ACAD, 3-demethylubiquinone-9 3-methyltransferase (COQ3), ubiquitin (UBI), ACUH, NADPH dehydrogenase (OYE), succinate/fumarate mitochondrial transporter (ACR1), and glutamine synthetase (GLN1). In general, the transcripts expression levels were similar to those identified by RDA and bioinformatic analyses (Fig. 3A).

The enzyme dihydropteroate synthase (DHPS) previously described as a target of sulfamethoxazole in fungi [45], and dihydrofolate reductase (DHFR), the last enzyme in the biosynthesis of folate cofactors, were not found by our RDA approach. These two enzymes were analyzed by qRT-PCR, revealing that the transcriptional levels of DHFR were only high after 6 h of exposure of *P. lutzii* yeast cells to sulfamethoxazole (Fig. 3B). However, DHPS was down regulated at all time points.

Transcripts level in *P. lutzii* yeast cells treated with sulfamethoxazole after internalization in macrophage cells

To investigate whether the regulated transcripts identified by the RDA method would be regulated during host-pathogen interactions, *P. lutzii* yeast cells were internalized by J774A.1 macrophage-like cells and the transcript levels were quantified. J774A.1 mouse macrophage-like cells were infected with *P. lutzii* and treated with sulfamethoxazole for 24 h, and qRT-PCR analysis was carried out for the genes ATP2, DHPS, and DHFR. ATP2 and DHPS were down-regulated in the library and qRT-PCR assays, and their expression levels were significantly lower after 24 h of infection in the sulfamethoxazole-treated cells (Fig. 3C).

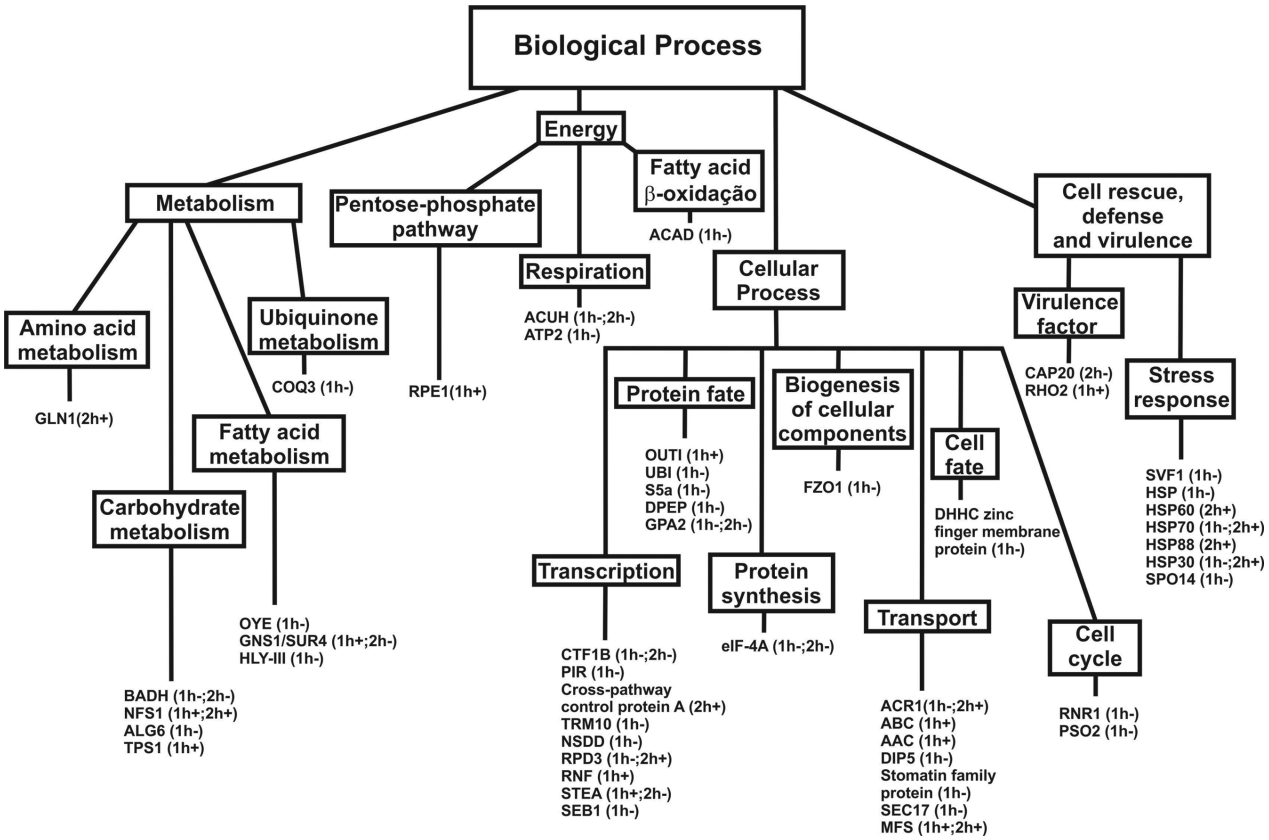

Figure 2. Distribution of genes responding to sulfamethoxazole in *P. lutzii*. The data are shown for a subset of genes that were significantly up- or down-regulated. The data were organized into various biological process using Functional Categories MIPS and GO tools. The parentheses show the time interval at which the alterations were detected, with "+" indicating up-regulation and "−" down-regulation. A complete list of all significant genes can be found in Table 1.

Similarly, DHFR was up-regulated in the qRT-PCR assays, and the level of DHRF was significantly higher after 24 h of infection in the presence of sulfamethoxazole.

MTT assay and Fluorescence microscopy

The MTT assay is an alternative method for measuring metabolic cellular function based on the transformation and colorimetric quantification of MTT. The respiratory chain [46] and other electron transport systems [47] reduce MTT and other tetrazolium salts and form non-water-soluble violet formazan crystals within the cell [48]. The amount of these crystals can be determined spectrophotometrically, and this serves as an estimate for the number of functional mitochondria and hence the number of living cells in the sample [49]. This assay has been used successfully to verify mitochondrial reduction capacity and viability [50]. The MTT method was used to verify the impact of sulfamethoxazole on *P. lutzii* mitochondrial activity. Sulfamethoxazole (0.01–1.28 mg/mL) produced a marked dose-dependent adverse effect on *P. lutzii* (Fig. 4A).

To further assess if sulfamethoxazole treatment leads to mitochondrial dysfunction, we used a fluorescence microscopy assay. We stained the *P. lutzii* yeast cells with 10 μM FUN after 24 and 48 h of treatment with three different concentrations of sulfamethoxazole (Fig. 4B and 4C). In metabolically active yeast cells, FUN-1 is transported to the vacuole and converted into a cylindrical intravacuolar structure (CIVS) that has a distinct orange-red fluorescence when excited by light from 470 nm to 590 nm. This process is mitochondrial-ATP dependent. The CIVS is completely abrogated by inhibition of mitochondrial cytochrome oxidase with sodium azide or sodium cyanide [51]. At 24 h, we observed a small decrease in activity at the subinhibitory concentrations tested. However, the impact of sulfamethoxazole at 48 h produced a notable dose dependent reduction that corroborates the MTT results.

Discussion

PCM is a granulomatous chronic mycoses [52]. Spontaneous cure is uncommon in PCM, except in some cases

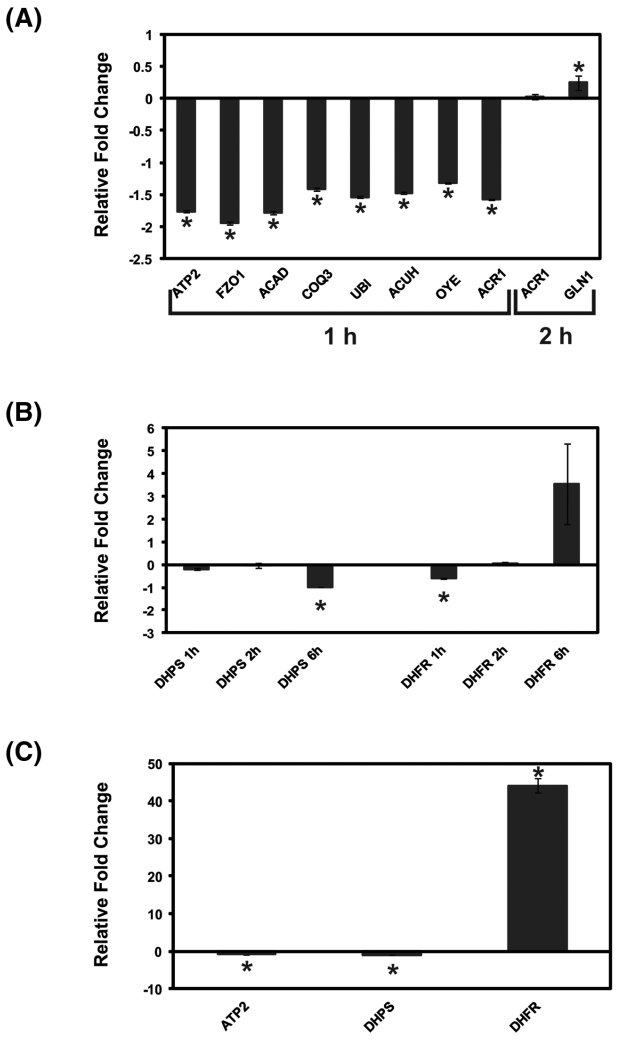

Figure 3. Expression profiles of ATP2, FZO1, ACAD, COQ3, UBI, ACUH, OYE, ACR1, GLN1, DHPS, and DHFR. **(A)** Gene expression profiles of *P. lutzii* yeast cells exposed to sulfamethoxazole after 1 and 2 h. **(B)** Expression profile of the genes DHPS and DHFR of *P. lutzii* yeast cell exposed to sulfamethoxazole after 1, 2 and 6 h. **(C)** Gene expression profile of *P. lutzii* yeast cells used to infect macrophages exposed to sulfamethoxazole after 24 h. Mean fold changes were calculated by a relative standard curve method using the untreated control samples as the calibrator. Each error bar represents the standard error of the mean (±SD) and significant -fold changes are denoted by asterisks in the figure ($^*P \leq 0.05$). The data were normalized with the transcript encoding the α-tubulin protein. Student´s t-test was used for statistical comparisons.

of primary lung infections [53]. Treatment of PCM includes the use of antifungal drugs and nutritional support, as well as the treatment of the sequelae of the disease and prevention of opportunistic diseases [54,55]. Although sulfamethoxazole has long been a mainstay of antimicrobial therapy, the mechanism of action of this drug against the *Paracoccidioides* genus has remained unknown. This study describes the cellular responses of *P. lutzii*, at a transcriptional level, to sulfamethoxazole exposure.

An RDA study was performed in *P. lutzii* yeast cells with or without exposure to sulfamethoxazole, and the results were confirmed by qRT-PCR and MTT assays. In addition, selected genes were also analyzed after infection with in co-cultures of *P. lutzii* and macrophages with or without sulfamethoxazole in the medium. The differentially expressed genes were involved in multiple biochemical functions. Our particular interest was the striking alterations in the regulation of energy-metabolism-related genes after sulfamethoxazole treatment: the down-regulated mitochondrial genes and the up-regulated genes associated with the biosynthesis of amino acids, purine and pyrimidine, which are involved in folate cofactor production.

Sulfa drugs inhibit *Saccharomyces cerevisiae* growth through competition with PABA, which is the precursor for the biosynthesis of folate cofactors that are active in the metabolism of single carbons [56]. Thus, one-carbon units that are carried and donated by tetrahydrofolate derivatives are essential for providing active one-carbon groups to the biosynthesis of methionine as well as to purines and thymidylate [57]. In *S. cerevivisiae*, as well as in other eukaryotes, both the cytoplasmic and mitochondrial compartments possess a set of enzymes that catalyze the interconversion of folate coenzymes. In the cytoplasm, the folate coenzymes participate in the synthesis of methionine, purines, and thymidylate. In the mitochondria, folate is required for the formylation of the initiator tRNA for mitochondrial protein synthesis [12]. In *S. cerevisiae*, one-carbon donors such as serine, glycine, and formate are able to cross the mitochondrial membrane [58]. Mitochondrial protein synthesis is required for maintenance of an intact mitochondrial genome in *S. cerevisiae* [59]. Moreover, inhibition of mitochondrial protein synthesis by the use of antifolates induces cytoplasmic respiration-deficient strains [60].

Our data allowed the identification of genes in the *P. lutzii* transcriptome that are impacted by sulfamethoxazole treatment. Interestingly, sulfamethoxazole-treated cells displayed significant reductions in protein expression levels by genes involved in mitochondrial functions. For instance, ACR1 was significantly down regulated after 1 h of exposure. In *S. cerevisiae*, Acr1p can specifically counter transport succinate and fumarate, which are known to be transporters for several substrates at the inner mitochondrial membrane [61]. ACR1 is thus strictly coregulated with the genes for key enzymes of the glyoxylate cycle and gluconeogenesis. Supporting the idea that Acr1p is the factor that transports succinate from the cytosol into the mitochondrial matrix in exchange for fumarate, ACR1 form an essential link between the glyoxylate and TCA cycles during growth on ethanol or acetate [62]. In addition, the expression of ACR1 is repressed by glucose [63]. ACR1 makes a small

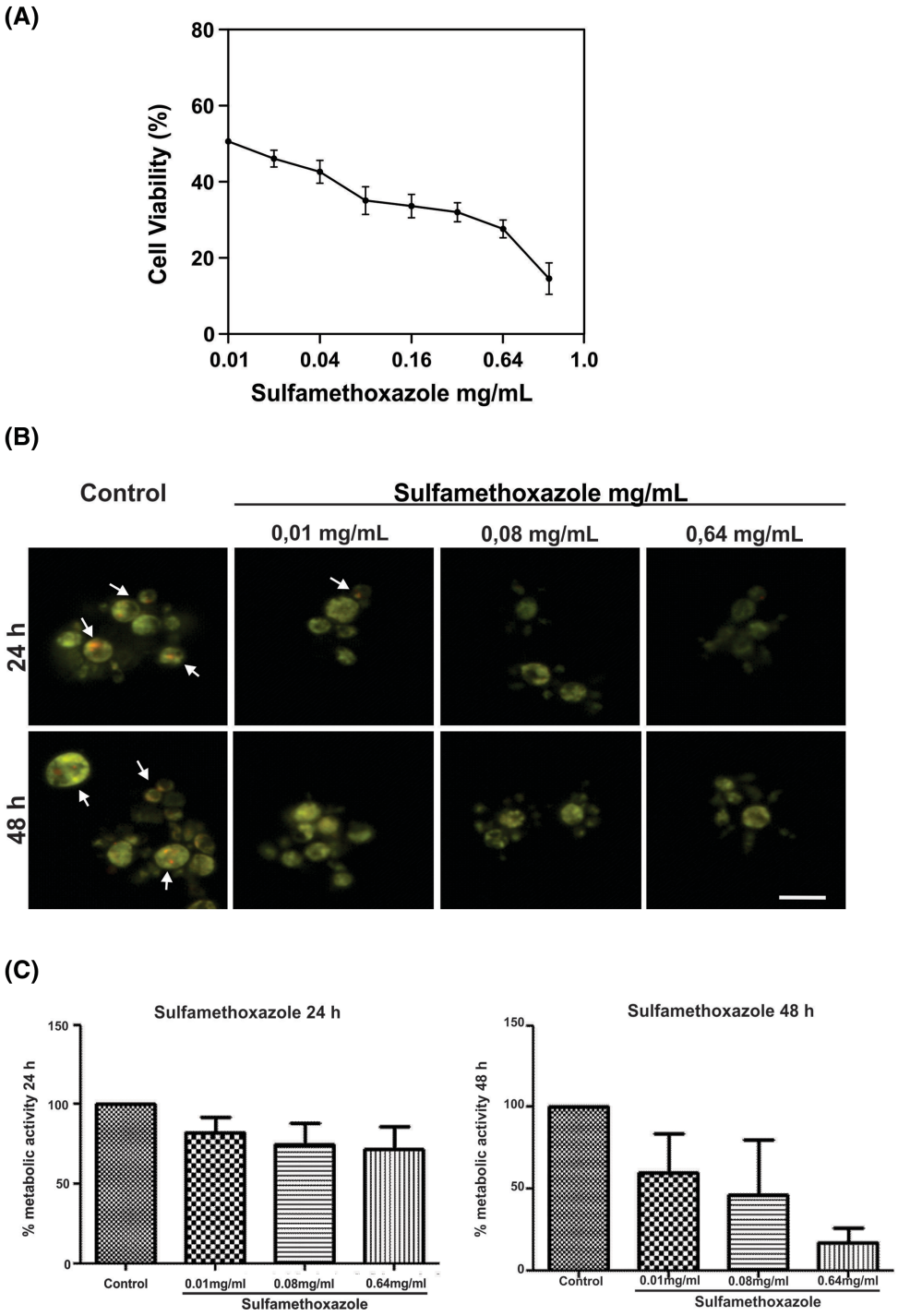

Figure 4. Effect of sulfamethoxazole on cell viability of *P. lutzii* as determined by MTT and Fluoresce microscopy. **(A)** *P. lutzii* yeast cells were maintained in culture medium (control), or incubated with various concentrations of sulfamethoxazole (0.01 – 1.28 mg/mL) for 120 h. The results are expressed as a percentage of cell viability by MTT reduction obtained through the mitochondrial activity in relation to control cells maintained in culture medium. Each value represents the mean ±SD from 3 experiments, performed in sextuplicate. **(B)** Mitochondrial function was assessed by FUN-1. The panels shows the staining with FUN-1 at three different concentrations of sulfamethoxazole at 24 h and 48 h. The white arrows indicate the formation of CIVS in metabolically active cells. Scale bar 20 μm. **(C)** The graphs represent the percentage of active cells in each condition at 24 h and 48 h of incubation. The graphs were normalized to 100% representing the activity of control cells. The experiments were repeated twice with similar results.

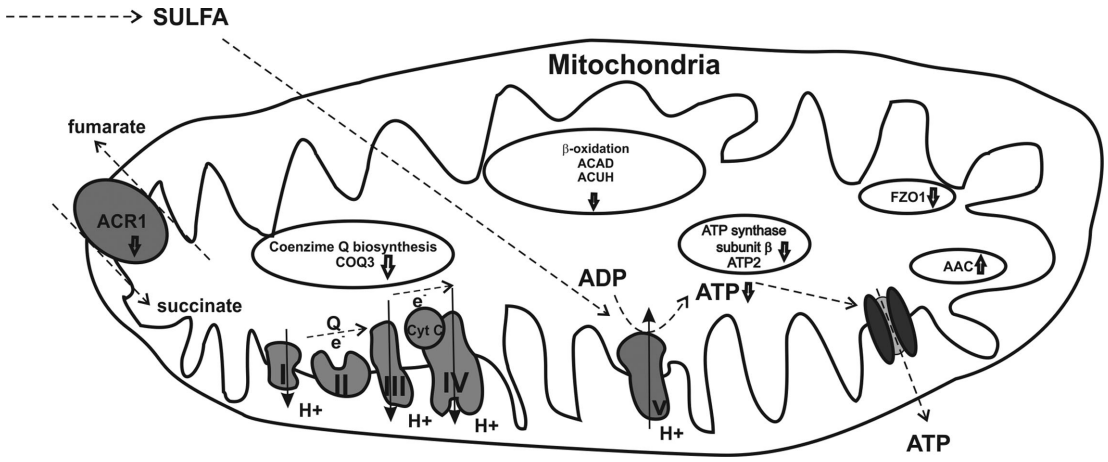

Figure 5. Hypothetical model for the mode of action of sulfamethoxazole against *P. lutzii*. The entry of sulfamethoxazole into the cell of *P. lutzii* causes the dissipation of the mitochondrial membrane potential by interfering with the biosynthesis of the electron transport chain due to the down-regulation of COQ3. The Krebs cycle and gluconeogenesis are also inhibited by low expression of ACR1. Sulfamethoxazole reduces the expression of the ATP2 subunit of F1F0-ATPase complex leading to a decrease in the production of ATP, and ATP levels are further reduced by the apparent up-regulation of the AAC. Additionally, down-regulation of β-oxidation enzymes reduces the overall fitness of the cell. Moreover, the low expression of FZO1 compromises mitochondrial biogenesis. The end result is the release of intracellular ATP as well as other nucleotides and molecules essential to energy storage. Hence, sulfamethoxazole is lethal to *P. lutzii* primarily through mitochondrial dysregulation.

contribution to the basal proton conductance of yeast mitochondria [64]. Thus, the down-regulation of ACR1 at 1 h could contribute to a dysregulated potential of membranes in *P. lutzii*, resulting in the dysfunction of the electron transport chain and ATP production.

The other major classes of down-regulated genes were those involved in ATP energy metabolism. Our data revealed that in *P. lutzii*, sulfamethoxazole significantly down regulated ATP2 expression. The F1F0-ATPase or ATP synthase rotates inside the cylinder formed by the six α and β subunits, and it compels the β subunits to undergo structural changes [65]. Because the expression of ATP synthase subunit β was decreased in the fungus treated with sulfamethoxazole, this could disrupt the production of ATP. In contrast to the suppression of ATP2, the expression level of the potential mitochondrial inner membrane ATP/ADP carrier protein (AAC) was increased after 1 h of sulfamethoxazole exposure. From these results, we postulate that mitochondrial ATP synthesis is reduced as a result of the inhibition of F1F0-ATPase and that the reduction in mitochondrial ATP is further accelerated by the transport of ATP from the mitochondrial matrix to the cytoplasm by increased expression of the AAC translocator.

The results from our work suggest that the efficiency of mitochondrial aerobic respiration would be decreased after sulfamethoxazole treatment. To test this hypothesis, functional analysis was carried out to measure mitochondrial activity in *P. lutzii* with or without exposure to sulfamethoxazole by using the MTT assay. The results demonstrated a reduction of *P. lutzii* mitochondrial activity in a dose-dependent manner, confirming the transcriptional data. The finding of a dose dependent reduction in FUN-1 staining further supports our finding that mitochondrial activity is affected by sulfamethoxazole.

Aspergillus nidulans contains both peroxisomal and mitochondrial β-oxidation pathways, and the genes encoding the proteins required for mitochondrial β-oxidation of even-numbered short chain fatty acids but not long chain fatty acids have been identified [66,67]. In *A. nidulans,* the catabolism of fatty acids begins with oxidation in the peroxisome to generate acetyl-CoA, which is transported into the mitochondria for its complete oxidation by the TCA. Acetyl moieties are imported into the mitochondria as esters with carnitine using the mitochondrial inner membrane carnitine/acylcarnitine carrier encoded by the ACUH gene [68]. Localization studies have clearly demonstrated the exclusive targeting of the ACUH gene product to the mitochondrial inner membrane [69,70]. In *P. lutzii,* the genes ACUH and ACAD were repressed after 1 h of exposure to sulfamethoxazole, which could compromise mitochondrial β-oxidation.

We propose a model for the mode of action of the sulfamethoxazole transcripts taking into account the available literature and our observations reported here. We could infer that sulfamethoxazole treatment results in (i) dissipation and permeabilization of the mitochondrial membrane potential, because COQ3 and ATP2 were down-regulated, and AAC is up-regulated; (ii) inhibition of gluconeogenesis precipitated by down-regulation of transporter ACR1; (iii) inhibition of β-oxidation by repression of ACAD and ACUH. The decrease in ATP production by F1F0-ATPase results from down-regulation of the ATP2 subunit. In sum,

the key steps in the antifungal mechanism of sulfamethoxazole involve a bioenergetic collapse of *P. lutzii* caused essentially by a decrease in mitochondrial ATP synthesis (Fig. 5).

Beyond the bioenergetic collapse caused by the repression of energy-metabolism-related genes, mitochondrial biogenesis in *P. lutzii* could be impaired by the downregulion of FZO1. Maintaining the capacity of the mitochondria to fuse normally is essential for the inheritance of mtDNA and for respiration. Fragmentation of the mitochondria leads to a loss of mtDNA and respiratory incompetence in *S. cerevisiae* [71]. Regulating levels of expression of Fzo1p is of critical importance; deletion or over expression of Fzo1p alters the mitochondrial fusion process resulting in fizzed or abnormal aggregated mitochondria, respectively [71,72].

GLN1 catalyzes the condensation of glutamate and ammonium to form glutamine, with concomitant hydrolysis of ATP [73]. Glutamate and glutamine are used as amino donors in all other biosynthetic reactions [74]. Glutamine can also be used as a sole nitrogen source [75]. GLN1 is involved in nitrogen metabolism via regulation by Gln3p or Gcn4p. Gcn4 is a transcription factor whose activity increases under amino acid starvation conditions in *S. cerevisiae* [76,77]. Moreover, the enzyme ρ-aminobenzoate synthase catalyzes the conversion of chorismate and glutamine, a product of GLN1, to an unidentified intermediate that is converted to PABA by a second enzyme [78]. PABA is essential for the biosynthesis of dihydrofolate, which in various forms participates in the synthesis of purines, pyrimidines, formylmethionyl-tRNA, and some amino acids and vitamins [79].

Finally, we suggest that in *P. lutzii* the product of GLN1 could be donating nitrogen for the synthesis of nucleic acids and amino acids, or even for the metabolism of purines or condensing with chorismate to produce the substrates for the biosynthetic pathway of folate cofactors.

Chorismate is a common intermediate in the biosynthesis of aromatic metabolites such as aromatic amino acids and folate cofactors [80]. The shikimate pathway starts with the condensation of erythrose-4-phosphate and phosphoenolpyruvate to 3-deoxy-D-arabino-heptulosonate-7-phosphate, which is converted to the branch point compound chorismate [81]. Chorismate is also a precursor for the aromatic amino acids tyrosine, phenylalanine, and tryptophan, which can polymerize to melanin, a virulence factor in *Paracoccidioides* genus. Erythrose-4-phosphate is the end product of pentose phosphate pathway, which is involved in the action of the enzyme ribulose-phosphate 3-epimerase (RPE1) that is over expressed in *P. lutzii* treated with sulfamethoxazole at 1 h. We propose that GLN1 and RPE1 could be participating in the production of substrates for the biosynthesis of folate cofactors, which is most likely a compensatory mechanism because, as already described for other fungi, sulfamethoxazole inhibits this pathway [45,10,11]. The pentose phosphate pathway is required for NADPH generation and nucleotide biosynthesis [82].

Although sulfamethoxazole inhibits the DHPS enzyme [45,10,11], the DHPS transcript was not found in our RDA analysis; however qRT-PCR analysis showed that the transcript level was reduced after 6 h of exposure to the compound as well as in co-cultures with macrophages when sulfamethoxazole was in the growth medium. An inhibitory effect at the transcript level to protein production by a compound not specifically targeting this process has been described in *Candida albicans* [83]. High concentrations of echinocandin, which inhibits the enzyme (1,3)-β-D-glucan synthase, suppressed *C. albicans* RNA synthesis consistent with an off-target effect. Interestingly, in contrast to DHPS, *P. lutzii* DHFR expression significantly increased after 6 h of exposure to sulfamethoxazole, and gene expression similarly increased in the co-cultures with macrophages exposed to the drug. Hence, in our system, we suggest that *P. lutzii* DHFR compensates for the small quantity of product formed by DHPS enzyme inhibitory competition with PABA and sulfamethoxazole.

Drug resistance is often associated with the over expression of genes encoding efflux pumps [84]. Two classes of efflux pumps, membrane transport proteins belonging either to the major facilitator superfamily (MFS) or to the ATP-binding cassette (ABC) superfamily, have been implicated in azole resistance [85]. The over expression of genes encoding efflux pumps is presumed to prevent accumulation of itraconazole in the fungal cell [86]. In *Candida glabrata,* azole resistance can occur with mitochondrial dysfunction. Cells with mitochondrial DNA deficiency and upregulated ABC transporter genes display increased resistance to azoles [87,88]. Our results suggest that this process could also occur in *P. lutzii* in response to sulfamethoxazole because the MFS and ABC transporters are up-regulated after 1 h of treatment.

The response of *P. lutzii* to sulfamethoxazole includes changing the profile of HSPs. HSPs are linked to cellular responses to various stressors such as changes in temperature and pH, the action of cytotoxic drugs, and oxidative stress [89–92]. The alterations in HSPs in response to sulfamethoxazole is are not surprising as these molecules are responsible for preventing damage to proteins [93].

Conclusions

This study is the first to our knowledge to analyze the changes in the *P. lutzii* transcriptional profile following

sulfamethoxazole exposure. The results indicated that sulfamethoxazole acts in *P. lutzii* as a competitor for the synthesis of amino acids, nucleic acids and precursors of the biosynthesis of folate cofactors resulting in the dysregulation of mitochondrial functions.

Our results demonstrate that sulfamethoxazole treatment impairs mitochondrial fitness and induces the overexpression of genes related to biosynthesis of amino acids and nucleic acids in *P. lutzii*, as well as genes linked to the biosynthesis of precursors in the synthesis of folate cofactors. As a whole, our findings regarding these biochemical processes involved in the mechanism of the action of sulfamethoxazole against *P. lutzii* provide significant insights that may lead to future drug design as well as provide new mechanistic information to clinicians caring for patients with PCM.

Acknowledgments

This work was supported by the International Foundation for Sciences (IFS), Conselho Nacional de Desenvolvimento Científico e Tecnológico (CNPq), Fundação de Amparo à Pesquisa do Estado de Goiás (FAPEG) and Financiadora de Estudos e Projetos (FINEP). Patrícia Fernanda Zambuzzi Carvalho and Amanda Gregorim Fernandes were supported by a fellowship from the Coordenação de Aperfeiçoamento de Pessoal de Nível Superior (CAPES).

Declaration of interest

The authors report no conflicts of interest. The authors alone are responsible for the content and the writing of the paper.

Supplementary material

Supplementary material is available at *Medical Mycology* online (http://www.mmy.oxfordjournals.org/).

References

1. Queiroz-Telles F, Escuissato DL. Pulmonary paracoccidioidomycosis. *Semin Respir Crit Care Med* 2011; **32**(6): 764–774.
2. Matute DR, McEwen JG, Puccia R et al. Cryptic speciation and recombination in the fungus *Paracoccidioides brasiliensis* as revealed by gene genealogies. *Mol Biol Evol* 2006; **23**(1): 65–73.
3. Theodoro RC, Teixeira MM, Felipe MS et al. Genus paracoccidioides: Species recognition and biogeographic aspects. *PLoS One* 2012; **7**(5): e37694.
4. Prado M, Silva MB, Laurenti R et al. Mortality due to systemic mycoses as a primary cause of death or in association with AIDS in Brazil: a review from 1996 to 2006. *Mem Inst Oswaldo Cruz* 2009; **104**(3): 513–521.
5. Bertini S, Colombo AL, Takahashi HK et al. Expression of antibodies directed to *Paracoccidioides brasiliensis* glycosphingolipids during the course of paracoccidioidomycosis treatment. *Clin Vaccine Immunol* 2007; **14**(2): 150–156.
6. Shikanai-Yasuda MA, Telles Filho FQ, Mendes RP et al. [Guidelines in paracoccidioidomycosis]. *Rev Soc Bras Med Trop* 2006; **39**(3): 297–310.
7. Travasso LR, Taborda CP. New advances in the development of a vaccine against paracoccidioidomycosis. *Front in Microbiol* 2012; **3**: 1–6.
8. Del Negro G. Ketoconazole in paracoccidioidomycosis. A long-term therapy study with prolonged follow-up. *Rev Inst Med Trop Sao Paul* 1982; **24**(1): 27–39.
9. Ferreira MS. Paracoccidioidomycosis. *Paediatr Respir Rev* 2009; **10**(4): 161–165.
10. Hanafy A, Uno J, Mitani H et al. In-vitro antifungal activities of sulfa drugs against clinical isolates of *Aspergillus* and *Cryptococcus* species. *Nihon Ishinkin Gakkai Zasshi* 2007; **48**(1): 47–50.
11. Patel OG, Mberu EK, Nzila AM et al. Sulfa drugs strike more than once. *Trends Parasitol* 2004; **20**(1): 1–3.
12. Appling DR. Compartmentation of folate-mediated one-carbon metabolism in eukaryotes. *FASEB J* 1991; **5**(12): 2645–2651.
13. Sun W, Park YD, Suqui JA et al. Rapid identification of antifungal compounds against Exserohilum rostratum using high throughput drug repurposing screens. *PLoS One* 2013; **8**(8): e70506.
14. Kim J, Cho YJ, Do E et al. A defect in iron uptake enhances the susceptility of *Cryptococcus neoformans* to azole antifungal drugs. *Fungal Genet Biol* 2012; **49**(11): 955–966.
15. Pastorian K, Hawel L, 3rd, Byus CV. Optimization of cDNA representational difference analysis for the identification of differentially expressed mRNAs. *Anal Biochem* 2000; **283**(1): 89–98.
16. Bailão AM, Schrank A, Borges CL et al. Differential gene expression by *Paracoccidioides brasiliensis* in host interaction conditions: representational difference analysis identifies candidate genes associated with fungal pathogenesis. *Microbes Infect* 2006; **8**(12–13): 2686–2697.
17. Bailão AM, Shrank A, Borges CL et al. The transcriptional profile of *Paracoccidioides brasiliensis* yeast cells is influenced by human plasma. *FEMS Immunol Med Microbil* 2007; **51**(1): 43–57.
18. Borges CL, Bailao AM, Bao SN et al. Genes potentially relevant in the parasitic phase of the fungal pathogen. *Paracoccidioides brasiliensis Mycopathologia* 2011; **171**(1): 1–9.
19. Silva MG, Schrank A, Bailao EFLC et al. The homeostasis of iron, copper and zinc in *Paracoccidioides brasiliensis*, *Cryptococcus neoformans var. grubi,* and *Cryptococcus gatii*: a comparative analysis. *Front Microbiol* 2011; **2**:49.
20. Bailão AM, Nogueira SV, Bonfim SMRC et al. Comparative transcriptome analysis of *Paracoccidioides brasiliensis* during in vitro adhesion to type I collagen and fibronectin: identification of potential adhesins. *Res Microbiol* 2012b; **163**(3): 182–191.
21. Bailão AM, Pereira M, Salem-Izacc SM et al. Transcript proffiling using ESTs from *Paracoccidioides brasiliensis* in model of infection. *Methods Mol Biol* 2012a; **845**: 381–396.
22. Hubank M, Schatz DG. Identifying differences in mRNA expression by representational difference analysis of cDNA. *Nucleic Acids Res* 1994; **22**(25): 5640–5648.
23. Cruz AH, Brock M, Zambuzzi-Carvalho PF et al. Phosphorylation is the major mechanism regulating isocitrate lyase activity in

Paracoccidioides brasiliensis yeast cells. *FEBS J* 2011; **278**(13): 2318–2332.
24. Tomazett PK, Felix CR, Lenzi HL et al. 1,3-beta-d-Glucan synthase of *Paracoccidioides brasiliensis*: recombinant protein, expression and cytolocalization in the yeast and mycelium phases. *Fungal Biol* 2010; **114**(10): 809–816.
25. Tomazett PK, Castro NS, Lenzi HL et al. Response of *Paracoccidioides brasiliensis* Pb01 to stressor agents and cell wall osmoregulators. *Fungal Biol* 2011; **115**(1): 62–69.
26. Zambuzzi-Carvalho PF, Cruz AH, Santos-Silva LK et al. The malate synthase of *Paracoccidioides brasiliensis* Pb01 is required in the glyoxylate cycle and in the allantoin degradation pathway. *Med Mycol* 2009; **47**(7): 734–744.
27. Fava-Netto C. Estudos quantitativos sobre a fixação de complementos na blastomicose sul-americana, com antígeno polissacarídico. *Arq Cir Clin Exp* 1995; **18**: 197–245.
28. Santos GD, Ferri PH, Santos SC et al. Oenothein B inhibits the expression of PbFKS1 transcript and induces morphological changes in *Paracoccidioides brasiliensis*. *Med Mycol* 2007; **45**(7): 609–618.
29. Restrepo A, Jimenez BE. Growth of *Paracoccidioides brasiliensis* yeast phase in a chemically defined culture medium. *J Clin Microbiol* 1980; **12**(2): 279–281.
30. Freshney R. *Culture of Animal Cells: A Manual of Basic Technique*. 5th ed. New York: Wiley Liss, 2005.
31. Ewing B, Hillier L, Wendl MC et al. Base-calling of automated sequencer traces using PHRED. I. Accuracy assessment. *Genome Res* 1998; **8**(3): 175–185.
32. *Crossmatch Program Database* [http://www.macvector.com/Assembler/trimmingwithcrossmatch.html].
33. Huang X, Madan A. CAP3: a DNA sequence assembly program. *Genome Res* 1999; **9**(9): 868–877.
34. *Laboratório de Biologia Molecular/UFG Database* [http://www.lbm.icb.ufg.br/joomlaLBM/].
35. *Blast2GO Program Database* [www.blast2go.com].
36. *GeneBank Database* [http://www.ncbi.nlm.nih.gov].
37. *Paracoccidioides Structural Genome Database* [http://www.broad.mit.edu/annotation/genome/paracoccidioides_brasiliensis/].
38. Apweiler R, Attwood TK, Bairoch A et al. The InterPro database, an integrated documentation resource for protein families, domains and functional sites. *Nucleic Acids Res* 2001; **29**(1): 37–40.
39. Kanehisa M, Goto S. KEGG: kyoto encyclopedia of genes and genomes. *Nucleic Acids Res* 2000; **28**(1): 27–30.
40. *MIPS Functional Catalog Database* [www.mips.helmholtz-muechen.de/genre/proj/yeast/].
41. Conesa A, Göts S, García-Gómez JM et al. Blast2GO: a universal tool for annotation, visualization and analysis in functional genomics research. *Bioinformatics* 2005; **21**(18): 3674–3676.
42. Götz S, García-Gómez JM, Terol J et al. High-throughput functional annotation and data mining with the Blast2GO suite. *Nucleic Acids Res* 2008; **36**(10): 3420–3435.
43. Bookout AL, Cummins CL, Mangelsdorf DJ et al. High-throughput real-time quantitative reverse transcription PCR. In: Ausubel FM, Brent R, Kingston RE et al.. *Current Protocols in Molecular Biology* 2006: 1581–1628.
44. Nguyen LN, Cesar GV, Le GT et al. Inhibition of *Candida parapsilosis* fatty acid synthase (Fas2) induces mitochondrial cell death in serum. *PLoS Pathog* 2012; **8**(8): e1002879.
45. Moukhlis R, Boyer J, Lacube P et al. Linking *Pneumocystis jiroveci* sulfamethoxazole resistance to the alleles of the DHPS gene using functional complementation in *Saccharomyces cerevisiae*. *Clin Microbiol Infect* 2010; **16**(5): 501–507.
46. Slater TF, Sawyer B, Straeuli U. Studies on succinate-tetrazolium reductase systems. III. Points of coupling of four different tetrazolium salts. *Biochim Biophys Acta* 1963; **77**: 383–393.
47. Liu Y, Peterson DA, Kimura H et al. Mechanism of cellular 3 -(4,5-dimethylthiazol-2-yl)-2,5-diphenyltetrazolium bromide (MTT) reduction. *J. Neurochem* 1997; **69**(2): 581–593.
48. Altman FP. Tetrazolium salts and formazans. *Prog Histochem Cytoche* 1976; **9**(3): 1–56.
49. Denizot F, Lang R. Rapid colorimetric assay for cell growth and survival. Modifications to the tetrazolium dye procedure giving improved sensitivity and reliability. *J Immunol Methods* 1986, **89**(2): 271–277.
50. Kim H, Yoon SC, Lee TY et al. Discriminative cytotoxicity assessment based on various cellular damages. *Toxicol Lett* 2009; **184**(1): 13–17.
51. Millard PJ, Roth BL, Thi HP et al. Development of the FUN-1 family of fluorescent probes for vacuole labeling and viability testing of yeasts. *Appl Environ Microbiol* 1997; **63**(7): 2897–2905.
52. Marques SA. Paracoccidioidomicose. *An Bras Dermatol* 1998; **73**(4): 455–469.
53. Miyaji M, Kamei K. Imported mycoses: an update. *J Infect Chemother* 2003; **9**(2): 107–113.
54. Mendes-Giannini MJ, Hanna SA, da Silva JL et al. Invasion of epithelial mammalian cells by *Paracoccidioides brasiliensis* leads to cytoskeletal rearrangement and apoptosis of the host cell. *Microbes Infect* 2004; **6**(10): 882–891.
55. Ramos ESM, Saraiva LE. Paracoccidioidomycosis. *Dermatol Clin* 2008; **26**(2): 257–269, vii.
56. Castelli LA, Nguyen NP, Macreadie IG. Sulfa drug screening in yeast: fifteen sulfa drugs compete with *p*-aminobenzoate in *Saccharomyces cerevisiae*. *FEMS Microbiol Lett* 2001; **199**(2): 181–184.
57. Cherest H, Thomas D, Surdin-Kerjan Y. Polyglutamylation of folate coenzymes is necessary for methionine biosynthesis and maintenance of intact mitochondrial genome in *Saccharomyces cerevisiae*. *J Biol Chem* 2000; **275**(19): 14056–14063.
58. Kastanos EK, Woldman YY, Appling DR. Role of mitochondrial and cytoplasmic serine hydroxymethyltransferase isozymes in de novo purine synthesis in *Saccharomyces cerevisiae*. *Biochemistry* 1997; **36**(48): 14956–14964.
59. Tzagoloff A, Shtanko A. Mitochondrial and cytoplasmic isoleucyl-, glutamyl- and arginyl-tRNA synthetases of yeast are encoded by separate genes. *Eur J Biochem* 1995; **230**(2): 582–586.
60. Wintersberger U, Hirsch J. Induction of cytoplasmic respiratory deficient mutants on yeast by the folic acid analogue, methotrexate. II. Genetic analysis of the methotrexate-induced petites. *Mol Gen Genet* 1973; **126**(1): 71–74.
61. Palmieri L, Lasorsa FM, De Palma A et al. Identification of the yeast ACR1 gene product as a succinate-fumarate transporter

essential for growth on ethanol or acetate. *FEBS Lett* 1997; **417**(1): 114–118.
62. Bojunga N, Kotter P, Entian KD. The s uccinate/fumarate transporter Acr1p of *Saccharomyces cerevisiae* is part of the gluconeogenic pathway and its expression is regulated by Cat8p. *Mol Gen Genet* 1998; **260**(5): 453–461.
63. Fernández M, Fernández E, Rodicio R. ACR1, a gene encoding a protein related to mitochondrial carriers, is essential for acetyl-CoA synthetase activity in *Saccharomyces cerevisiae*. *Mol Gen Genet* 1994; **242**(6): 727–735.
64. Roussel D, Harding M, Runswick MJ et al. Does any yeast mitochondrial carrier have a native uncoupling protein function? *J Bioenerg Biomembr* 2002; **34**(3): 165–176.
65. Komatsu T, Salih E, Helmerhorst EJ et al. Influence of histatin 5 on *Candida albicans* mitochondrial protein expression assessed by quantitative mass spectrometry. *J Proteome Res* 2011; **10**(2): 646–655.
66. Maggio-Hall LA, Keller NP. Mitochondrial beta-oxidation in *Aspergillus nidulans*. *Mol Microbiol* 2004; **54**(5): 1173–1185.
67. Maggio-Hall LA, Lyne P, Wolff JA et al. A single acyl-CoA dehydrogenase is required for catabolism of isoleucine, valine and short-chain fatty acids in *Aspergillus nidulans*. *Fungal Genet Biol* 2008; **45**(3): 180–189.
68. De Lucas JR, Domínguez AI, Valenciano S et al. The acuH gene of *Aspergillus nidulans,* required for growth on acetate and long-chain fatty acids, encodes a putative homologue of the mammalian carnitine/acylcarnitine carrier. *Arch Microbiol* 1999; **171**(6): 386–396.
69. Ramón De Lucas J, Martínez O, Pérez P et al. The *Aspergillus nidulans* carnitine carrier encoded by the acuH gene is exclusively located in the mitochondria. *FEMS Microbiol Lett* 2001; **201**(2): 193–198.
70. van Roermund CW, Hettema EH, van den Berg M et al. Molecular characterization of carnitine-dependent transport of acetyl-CoA from peroxisomes to mitochondria in *Saccharomyces cerevisiae* and identification of a plasma membrane carnitine transporter, Agp2p. *EMBO J* 1999; **18**(21): 5843–5852.
71. Hermann GJ, Thatcher JW, Mills JP et al. Mitochondrial fusion in yeast requires the transmembrane GTPase Fzo1p. *J Cell Biol* 1998; **143**(2): 359–373.
72. Fritz S, Weinbach N, Westermann B. Mdm30 is an F-box protein required for maintenance of fusion-competent mitochondria in yeast. *Mol Biol Cell* 2003; **14**(6): 2303–2313.
73. Eisenberg D, Gill HS, Pfluegl GM et al. Structure-function relationships of glutamine synthetases. *Biochim Biophys Acta* 2000; **1477**(1–2): 122–145.
74. Magasanik B. Regulation of nitrogen utilization. In: Jones EW, Pringle JR, Broach JR. *The Molecular Biology of the Yeast Saccharomyces cerevisiae: Gene Expression*, **vol 2**. New York: Cold Spring Harbor Laboratory Press, 1992: 283–317.
75. Cogoni C, Valenzuela L, Gonzalez-Halphen D et al. *Saccharomyces cerevisiae* has a single glutamate synthase gene coding for a plant-like high-molecular-weight polypeptide. *J Bacteriol* 1995; **177**(3): 792–798.
76. Daugherty JR, Rai R, el Berry HM et al. Regulatory circuit for responses of nitrogen catabolic gene expression to the GLN3 and DAL80 proteins and nitrogen catabolite repression in *Saccharomyces cerevisiae*. *J Bacteriol* 1993; **175**(1): 64–73.
77. Dever TE, Feng L, Wek RC et al. Phosphorylation of initiation factor 2 alpha by protein kinase GCN2 mediates gene-specific translational control of GCN4 in yeast. *Cell* 1992; **68**(3): 585–596.
78. Nichols BP, Seibold AM, Doktor SZ. para-aminobenzoate synthesis from chorismate occurs in two steps. *J Biol Chem* 1989; **264**(15): 8597–8601.
79. Bognar AL, Osborne C, Shane B et al. Folylpoly-gamma-glutamate synthetase-dihydrofolate synthetase. Cloning and high expression of the *Escherichia coli folC* gene and purification and properties of the gene product. *J Biol Chem* 1985; **260**(9): 5625–5630.
80. Floss HG, Onderka DK, Carroll M. Stereochemistry of the 3-deoxy-D-arabino-heptulosonate 7-phosphate synthetase reaction and the chorismate synthetase reaction. *J Biol Chem* 1972; **247**(3): 736–744.
81. Knaggs AR. The biosynthesis of shikimate metabolites. *Nat Prod Rep* 2001; **18**(3): 334–355.
82. Hahn-Hägerdal B, Karhumaa K, Jeppsson M et al. Metabolic engineering for pentose utilization in *Saccharomyces cerevisiae*. *Adv Biochem Eng Biotechno* 2007; **108**: 147–177.
83. Liu J, Bolstad DB, Bolstad ESD et al. Towards new antifolates targeting eukaryotic opportunisitic infections. *Eukaryotic Cell* 2009; **8**(4): 483–486.
84. Lupetti A, Danesi R, Campa M et al. Molecular basis of resistance to azole antifungals. *Trends Mol Med* 2002; **8**(2): 76–81.
85. Ghannoum MA, Rice LB. Antifungal agents: mode of action, mechanisms of resistance, and correlation of these mechanisms with bacterial resistance. *Clin Microbiol Rev* 1999; **12**(4): 501–517.
86. Diao Y, Zhao R, Deng X et al. Transcriptional profiles of *Trichophyton rubrum* in response to itraconazole. *Med Mycol* 2009; **47**(4): 237–247.
87. Ferrari S, Sanguinetti M, De Bernardis F et al. Loss of mitochondrial functions associated with azole resistance in *Candida glabrata* results in enhanced virulence in mice. *Antimicrob Agents Chemother* 2011; **55**(5): 1852–1860.
88. Ferrari S, Sanguinetti M, Torelli R et al. Contribution of CgPDR1-regulated genes in enhanced virulence of azole-resistant *Candida glabrata*. *PLoS One* 2011; **6**(3): e17589.
89. Matuszewska E, Kwiatkowska J, Kuczynska-Wisnik D et al. *Escherichia coli* heat-shock proteins IbpA/B are involved in resistance to oxidative stress induced by copper. *Microbiology* 2008; **154**(6): 1739–1747.
90. Kalmar B, Greensmith L. Induction of heat shock proteins for protection against oxidative stress. *Adv Drug Deliv Rev* 2009; **61**(4): 310–318.
91. Dempsey NC, Ireland HE, Smith CM et al. Heat Shock Protein translocation induced by membrane fluidization increases tumor-cell sensitivity to chemotherapeutic drugs. *Cancer Lett* 2010; **296**(2): 257–267.
92. Squina FM, Leal J, Cipriano VT et al. Transcription of the *Neurospora crassa* 70-kDa class heat shock protein genes is modulated in response to extracellular pH changes. *Cell Stress Chaperones* 2010; **15**(2): 225–231.
93. Gupta RS, Golding GB. Evolution of HSP70 gene and its implications regarding relationships between archaebacteria, eubacteria, and eukaryotes. *J Mol Evol* 1993; **37**(6): 573–582.